2-7-2006

Self-consistent local GW method: Application to 3*d* and 4*d* metals

Kirill D. Belashchenko
University of Nebraska-Lincoln, belashchenko@unl.edu

Vladimir P. Antropov
Ames Laboratory, US Department fo Energy, antropov@ameslab.gov

N.E. Zein
Russian Research Center "Kurchatov Institute," Moscow 123182, Russia

Self-consistent local GW method: Application to 3*d* and 4*d* metals

K. D. Belashchenko
Department of Physics and Astronomy and Center for Materials Research and Analysis, University of Nebraska-Lincoln, Lincoln, Nebraska 68588, USA

V. P. Antropov
Condensed Matter Physics, Ames Laboratory, Ames, Iowa 50011, USA

N. E. Zein
Russian Research Center "Kurchatov Institute," Moscow 123182, Russia

(Received 1 September 2005; revised manuscript received 14 November 2005; published 7 February 2006)

The spectral densities for 3*d* and 4*d* transition metals are calculated using the simplified version of the self-consistent GW method employing the local (one-site) approximation and the self-consistent quasiparticle basis set. The results are compared with those given by the traditional local density approximation (LDA) and also with experimental x-ray photoemission and inverse photoemission spectra. While no systematic improvements over LDA are observed, this fully self-consistent many-body technique generates quite reasonable results and can serve as a practical prototype for further development of the many-body electronic structure theory.

DOI: 10.1103/PhysRevB.73.073105 PACS number(s): 71.10.−w, 71.20.Be, 71.15.Qe

I. INTRODUCTION

The electronic properties of many solids are described reasonably well by the local density approximation (LDA) of the density functional theory (DFT),[1] which is essentially a single-particle theory based on a drastic simplification of the full many-body problem. However, the LDA fails in materials exhibiting strong spatial electronic correlations, temporal correlations (retardation) associated with Coulomb screening, etc. These fundamental difficulties are extremely hard to overcome within the DFT without sacrificing the first-principles approach.

One of the methods used to correct the deficiencies of LDA in the description of excited states in metals and semiconductors is the GW approximation (GWA).[2,3] The GWA usually improves the band gaps in semiconductors and insulators;[3] in metals it may provide information on the quasiparticle lifetimes and renormalization which is absent in the DFT.[3,4] However, in most treatments used until recently, the GWA was employed in a non-self-consistent fashion, by using unrenormalized Green's functions constructed from the Kohn-Sham eigenstates obtained in LDA. This approach is easier to implement, but it is internally inconsistent: since its self-energy cannot be obtained by variation of any Luttinger-Ward functional,[5] it violates basic conservation laws,[6] and the results depend on the approximation used to solve the Kohn-Sham equations. On the other hand, studies of the homogeneous electron gas have shown that self-consistency worsens the agreement of the GWA results with experiment at typical metallic densities,[7] highlighting the limitations of GWA which is formally accurate only in the high-density limit.

Recently, several self-consistent realizations of the GWA were demonstrated. One of them[8] was tailored for transition metals and employed the one-site approximation (OSA) for the self-energy which is justified by the localized character of *d*-electron wave functions and by the fact that the static Coulomb interaction is efficiently screened. Some spin-selective diagrams beyond GW were also included. The results for Fe and Ni were quite reasonable, although no improvement was obtained compared to LDA. Later, the accuracy of the OSA for transition metals was demonstrated explicitly by cluster GW calculations.[9] Although the choice of GW diagrams is unjustified for the homogeneous electron gas at typical metallic densities and likewise for semiconductors (the diagrams that are left out do not contain any small parameter), it was noted that the situation may be better in transition metals, because high orbital degeneracy provides an additional enhancement to the diagrams with the largest number of closed electron loops, thereby favoring the GW set.[8] On the other hand, OSA makes self-consistent calculations much easier.

Another realization[10] using GW set with the full **k** dependence of the self-energy was applied to elemental semiconductors. It was found that self-consistency and accurate treatment of core electrons improve the agreement with experiment for the band gaps in Si and Ge.

A simplification of GWA neglecting the renormalization factor Z was also suggested.[11] For many insulators and semiconductors this method predicts band gaps in very good agreement with experiment.[12] Self-consistency was found to be essential for this agreement.

While the adequacy of GWA for the studies of metals and semiconductors has not been firmly established from the point of view of the many-body theory, this method may be regarded as a practical step toward a consistent Green's function-based scheme. Therefore, it is important to ascertain the degree of accuracy of this approximation for different materials. This is especially desirable for transition metals where, as noted above, there are reasons why GWA may work better than in the homogeneous electron gas. In this paper we calculate the conduction-band spectral densities for

all elemental $3d$ and $4d$ metals using the self-consistent one-site GW approach and compare them both with experimental spectroscopic data and with standard LDA results.

II. SELF-CONSISTENT GW METHOD IN THE ONE-SITE APPROXIMATION

The technique used in this paper was introduced in Ref. 8 and further tested in Ref. 9. Here we describe some points in more detail.

The self-energy $\Sigma = \delta\Phi/\delta G$ is obtained from the Luttinger-Ward generating functional Φ defined by the set of skeleton graphs.[5] The Hartree diagram gives the local contribution $V_H(\mathbf{r})$, and the exchange diagram contributes $\Sigma_x = V(\mathbf{r}-\mathbf{r}')\int \mathrm{Im}\, G(\mathbf{r},\mathbf{r}',\epsilon)d\epsilon/\pi$, where V is the Coulomb potential. The total contribution of the remaining GW sequence (the "correlation term") is

$$\Sigma_c(\mathbf{r},\mathbf{r}',\epsilon) = -\int G(\mathbf{r},\mathbf{r}',\epsilon-\omega)V(\mathbf{r}-\mathbf{r}_1) \times \Pi(\mathbf{r}_1,\mathbf{r}_2,\omega)W(\mathbf{r}_2,\mathbf{r}',\omega)d\mathbf{r}_1 d\mathbf{r}_2 \frac{d\omega}{2\pi i}. \quad (1)$$

Here W is the effective (screened Coulomb) interaction defined by the Dyson equation

$$W = V - \int V(\mathbf{r}-\mathbf{r}_1)\Pi(\mathbf{r}_1,\mathbf{r}_2,\epsilon)W(\mathbf{r}_2,\mathbf{r}',\epsilon)d\mathbf{r}_1 d\mathbf{r}_2, \quad (2)$$

and Π is the polarization operator

$$\Pi(\mathbf{r},\mathbf{r}',\omega) = -\int G(\mathbf{r},\mathbf{r}',\epsilon)G(\mathbf{r}',\mathbf{r},\epsilon+\omega)\frac{d\epsilon}{2\pi i}. \quad (3)$$

The integration contour in Eqs. (1) and (3) is directed along the imaginary axis and embraces the cut on the real axis from the Fermi energy E_F to the external energy. The GW approximation may be modified by the inclusion of vertex corrections in the polarization operator (3) which may sometimes improve the results.

The calculations are drastically simplified by the use of the one-site approximation[8] (OSA), in which the self-energy is calculated only on one lattice site neglecting all matrix elements connecting different sites. This approximation is conceptually similar to the highly successful single-site dynamical mean-field theory (DMFT).[13] It is particularly reasonable for transition metals for two reasons: first, because the d-electron wave functions are fairly localized, which makes the intersite exchange integrals small already at the Hartree-Fock level and, second, because static Coulomb interaction in metals is effectively screened at the interatomic distance. The validity of OSA was checked for different materials, and it was found to be very accurate for transition metals.[9]

In OSA the self-energy depends on energy and on the coordinates $\mathbf{r}$, $\mathbf{r}'$ belonging to the same unit cell. In order to implement OSA we need to choose an appropriate on-site basis. Considering the successful description of closely packed solids by the atomic sphere approximation within the linear muffin-tin orbital method (LMTO-ASA), we use the minimal set with one basis function for each angular momentum l and its projection m, along with its energy derivative (below we denote $L \equiv lm$). The radial basis functions $\phi_l(r)$ satisfy the equation

$$\left[\epsilon_l + \frac{\Delta_l}{2} - V_{\mathrm{H}} - \hat{\Sigma}_l(\epsilon_l)\right]\phi_l(r) = 0, \quad (4)$$

where Δ_l is the radial part of the Laplasian, and $\hat{\Sigma}_l$ is an integral radial operator whose kernel is obtained from $\mathrm{Re}\hat{\Sigma}$ by projecting onto the l subspace

$$\Sigma_l(r,r',\epsilon) = \frac{1}{2l+1}\sum_m \int Y_L(\hat{r})\mathrm{Re}\,\Sigma_{xc}(\mathbf{r},\mathbf{r}',\epsilon)Y_L(\hat{r}')dodo', \quad (5)$$

where we denoted $\Sigma_{xc} \equiv \Sigma_x + \Sigma_c$, Y_L are the spherical harmonics, and integration is over the directions of $\mathbf{r}$, $\mathbf{r}'$. The operator $\hat{\Sigma}_l$ may be represented as the sum of its local part $\Sigma_l^{(l)}(r)$ similar to an external potential, and a nonlocal part $\hat{\Sigma}_l^{(n)}$ whose operation on ϕ_l gives a linear combination of $\phi_{l'}$ with $l' \neq l$.

Similar to the LMTO-ASA method, the solutions of Eq. (4) for each l are only found at one energy ϵ_l chosen at the center of gravity of the occupied part of the given band. We may safely discard the imaginary part of the self-energy operator because it is small in the vicinity of E_F where ϵ_l is usually chosen. Thus, our radial basis functions are real. The nonlocal equation (4) is solved by iterations. The $(n+1)$-th iteration ϕ_l^{n+1} for the solution is obtained using auxiliary functions f_l and g_l defined as

$$\left[\epsilon_l + \frac{\Delta_l}{2} - V_{\mathrm{H}} - \Sigma_l^{(l)}(r)\right]f_l(r) = \hat{\Sigma}_l^{(n)}(\epsilon_l)\phi_l^n, \quad (6)$$

$$\left[\epsilon_l + \frac{\Delta_l}{2} - V_{\mathrm{H}}\right]g_l(r) = 0 \quad (7)$$

according to $\phi_l^{n+1}(r) = f_l(r) + Ag_l(r)$, where A is found by normalizing ϕ_l^{n+1}. Just as in the LMTO method, we also compute the energy derivative $\dot{\phi}_l \equiv \partial\phi_l/\partial\epsilon$:

$$\left[\epsilon_l + \frac{\Delta_l}{2} - V_{\mathrm{H}} - \hat{\Sigma}_l(\epsilon_l)\right]\dot{\phi}_l = -\phi_l + \frac{\partial\hat{\Sigma}_l(\epsilon_l)}{\partial\epsilon_l}\phi_l. \quad (8)$$

To stabilize the solution of the Schrödinger equation (4), we added the exchange with the nearest-neighbor cells to Σ_{xc}. The corresponding matrix element was subtracted from Green's function (9) below.

With the on-site self-energy $\Sigma_{\mathrm{xc}}(\mathbf{r},\mathbf{r}',\epsilon)$ defined for r, r' within the same unit cell, we can calculate its matrix elements between the muffin-tin "eigenfunctions" $\chi_{\mathbf{k}\nu}$ that are linear combinations of ϕ_l and $\dot{\phi}_l$. Due to the $\mathbf{k}$ dependence of $\chi_{\mathbf{k}\nu}$, the self-energy also acquires $\mathbf{k}$ dependence, just as the matrix elements of the local potential in LDA. Finally, on-site Green's function is found by integration using the tetrahedron method

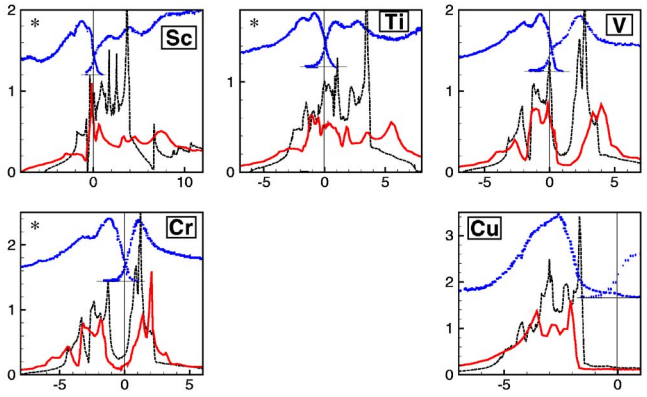

FIG. 1. (Color online) Spectral densities obtained in GW-OSA (solid red lines), LDA densities of states (dashed black lines), and experimental XPS and BIS spectra (dotted blue lines shifted up) for nonmagnetic 3*d* metals. Elements for which the crystal structure was not experimental are marked by a star in the upper left corner. In all graphs the *x* axis shows energy referenced from E_F in eV, and the *y* axis denotes the spectral density in eV^{-1} for the calculated curves.

$$G(\mathbf{r},\mathbf{r}',\varepsilon)=\sum_{\mathbf{k}\nu}\frac{\chi^R_{\mathbf{k}\nu}(\mathbf{r})\chi^L_{\mathbf{k}\nu}(\mathbf{r}')}{\varepsilon-\lambda_{\mathbf{k}\nu}}, \tag{9}$$

where $\chi^R_{\mathbf{k}\nu}$ and $\chi^L_{\mathbf{k}\nu}$ are right and left eigenvectors, and $\lambda_{\mathbf{k}\nu}$ the eigenvalues of the non-Hermitian operator $H_0+\Sigma_{\mathrm{xc}}$, where H_0 is the Hartree Hamiltonian. Equation (9) imposes the locality condition and is equivalent to the self-consistency relation of the DMFT.[13]

III. CONDUCTION BAND SPECTRAL DENSITIES OF TRANSITION METALS

Using the GW technique described above, we calculated the spectral densities $N(\epsilon)=-\mathrm{Tr}\ \mathrm{Im}\ G(\epsilon)/\pi$ for elemental 3*d* and 4*d* metals, where LDA has long been the only appropriate approximation. We used the fcc structure for hcp elements (Sc, Ti, Y, Zr, Tc, Ru, Co) and the bcc structure for Mn. All atomic volumes were taken from experiment. Cr was treated within the single bcc cell, and hence was nonmagnetic. The Brillouin zone integrations were performed by tetrahedron method on a grid with 16 points along each reciprocal lattice vector.

The first iteration was started from the LDA potential, and at each iteration the nonlocal self-energy was mixed with this potential with a gradually increasing weight, leaving only Σ_{xc} in the end. In the final state the magnitude of Σ_{xc} differs by about 40% from its initial LDA value. The iterational procedure is rather stable in all metals except Ni where the magnetic moment is very sensitive to the details of the calculation.

The results are shown in Figs. 1–3 along with the LDA densities of states (DOS) and the experimental XPS and BIS spectra taken from Refs. 14 and 15. Strictly speaking, comparison with experiment requires the calculation of the corresponding matrix elements, but we believe that in the present context some qualitative conclusions can be drawn based on the spectral densities alone.

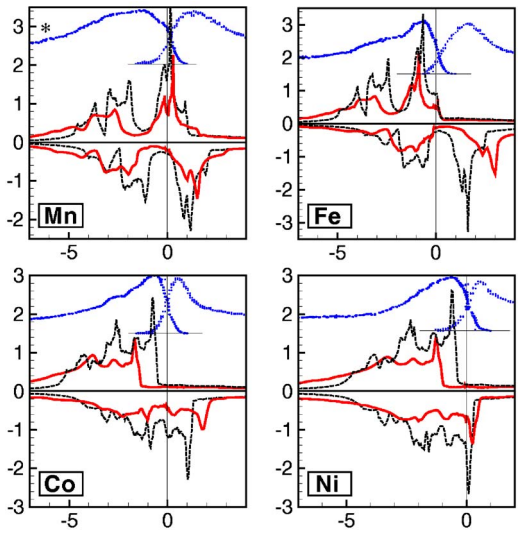

FIG. 2. (Color online) Same as in Fig. 1 but for magnetic 3*d* elements. The data for majority-spin and minority-spin electrons are plotted as positive and negative values, respectively.

The difference between the LDA DOS and GW spectral density may be generally summarized as follows. The conduction band widens as all DOS features are pushed away from E_F; this outward shift is roughly proportional to the distance from E_F. Moreover, all DOS features are increasingly smeared out due to the decreasing quasiparticle lifetime as the distance from E_F increases. Substantial spectral weight is transferred from the quasiparticle states to the incoherent "tail" extending far below E_F.

The LDA DOS for *d* metals is typically too small to account for the measured electronic specific heat $C=\gamma T$. As seen from Figs. 1–3 the GW spectral density at E_F is generally smaller compared to LDA. Although to obtain γ we have to remove the renormalization factor Z from Im G, the GW method does not improve the overall agreement with specific heat measurements.

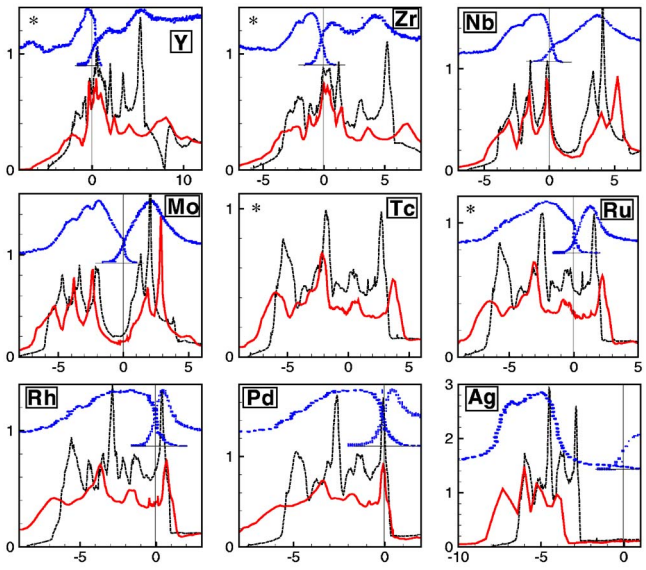

FIG. 3. (Color online) Same as in Fig. 1 but for 4*d* metals.

The difference between the GW and LDA spectra is most notable for early transition metals (treated here in the fcc structure), where the strongest unoccupied peaks given by LDA are almost completely smeared out in GW. Notably, the worst agreement with experiment for the LDA spectra is observed for the same elements. In particular, the position of the Fermi level obtained in LDA for hcp Sc and Y appears to be off by nearly 1 eV.[14]

The agreement between LDA and GW improves as we move to later transition metals and as the fcc structure is replaced by the bcc one. In V and Nb the GW and LDA curves are already quite similar except for the shift of the unoccupied d peak by 1.5–2 eV to higher energies.

As in LDA, the $3d$ metals from Mn to Ni were magnetic in our calculation. For simplicity, we used the bcc structure for Mn, and also the fcc structure for Co (this structure is stable in thin films). As it is seen in Fig. 1, the general features of the GW spectral density described above are observed in these metals as well. In general, the GW description also gives a reasonable exchange splitting and magnetic moment. We obtained the moments of $0.9\mu_B$ for Mn compared to $1.03\mu_B$ in LDA, $2.3\mu_B$ for Fe compared to $2.25\mu_B$ in LDA, and $1.85\mu_B$ for fcc Co compared to $1.62\mu_B$ in LDA. From these results it is clear that there is no systematic trend for GW to give larger or smaller magnetic moments compared to LDA. The magnetic moment in Ni is rather sensitive to various details of the calculation, and proper convergence turned out to be problematic. We believe that the approach based on Matsubara Green's functions is necessary to avoid this problem. Apart from the exchange splitting, the shape of the spectrum is quite stable. We also note that the magnetic moment is expected to be sensitive to the choice of the skeleton graph set.

As an example of the general trend of band dilatation off the Fermi level, the distance from E_F to the upper edge of the fully occupied d-band in Cu and Ag is notably larger in GW compared to LDA, which results in a better agreement with experimental XPS spectra. On the other hand, we also observe a rather strong upward shift of the unoccupied peak in V, Nb, Fe, and Mo in obvious disagreement with the BIS spectra. This shift is more pronounced compared to the downward shift of the occupied states at a similar distance from E_F.

The results presented above demonstrate that the self-consistent GW approach with one-site approximation provides a reasonable description of transition metals. For $3d$ and $4d$ systems the GW spectral density is generally similar to the LDA density of states, while the GW approach includes typical Fermi-liquid effects such as finite quasiparticle lifetime and self-consistent renormalization. The preliminary comparison of the GW-OSA results with experiment is satisfactory and clearly indicates its problems that need improvement, namely, the exchange splitting in ferromagnets, value of $N(E_F)$, and the unoccupied peak position which is too high for some metals. The first two deficiencies are common with LDA. In general, the presented technique based on the Luttinger-Ward functional is a practical alternative to DFT and can serve as a reasonable starting point for more sophisticated methods.

ACKNOWLEDGMENTS

This work was completed utilizing the Research Computing Facility of the University of Nebraska-Lincoln. This work was partially carried out at Ames Laboratory, which is operated for the U.S. Department of Energy by Iowa State University under Contract No. W-7405-82. This work was supported by the Director for Energy Research, Office of Basic Energy Sciences of the U.S. Department of Energy. N.E.Z. acknowledges support from the Council for the Support of Leading Scientific Schools of Russia under Grant No. NS-1572.2003.2.

[1] P. Hohenberg and W. Kohn, Phys. Rev. **136**, B864 (1964); W. Kohn and L. J. Sham, Phys. Rev. **140**, A1133 (1965).
[2] L. Hedin, Phys. Rev. **139**, A796 (1965).
[3] F. Aryasetiawan and O. Gunnarsson, Rep. Prog. Phys. **61**, 237 (1998).
[4] V. M. Silkin, E. V. Chulkov, and P. M. Echenique, Phys. Rev. B **68**, 205106 (2003), and references therein.
[5] J. M. Luttinger and J. C. Ward, Phys. Rev. **118**, 1417 (1960).
[6] G. Baym and L. P. Kadanoff, Phys. Rev. **124**, 287 (1961); G. Baym, *ibid.* **127**, 1391 (1962).
[7] B. Holm and U. von Barth, Phys. Rev. B **57**, 2108 (1998).
[8] N. E. Zein and V. P. Antropov, Phys. Rev. Lett. **89**, 126402 (2002).
[9] N. E. Zein, S. Y. Savrasov, and G. Kotliar, cond-mat/0511064 (unpublished).
[10] W. Ku and A. G. Eguiluz, Phys. Rev. Lett. **89**, 126401 (2002).
[11] S. V. Faleev, M. van Schilfgaarde, and T. Kotani, Phys. Rev. Lett. **93**, 126406 (2004).
[12] M. van Schilfgaarde, T. Kotani, and S. V. Faleev, cond-mat/0510408 (unpublished).
[13] A. Georges, G. Kotliar, W. Krauth, and M. Rozenberg, Rev. Mod. Phys. **68**, 13 (1996).
[14] A. G. Narmonev and A. I. Zakharov, Phys. Met. Metallogr. **65**, 315 (1988).
[15] W. Speier, J. C. Fuggle, R. Zeller, B. Ackermann, K. Szot, F. U. Hillebrecht, and M. Campagna, Phys. Rev. B **30**, 6921 (1984).